Sleep, J. A., & Boyer, P. D. (1978) *Biochemistry 17*, 5417–5422.
Sleep, J. A., Hackney, D. D., & Boyer, P. D. (1980) *J. Biol. Chem. 255*, 4094–4099.
Stein, L. A., Schwartz, R. P., Chock, P. B., & Eisenberg, E. (1979) *Biochemistry 18*, 3895–3909.
Stein, L. A., Chock, P. B., & Eisenberg, E. (1984) *Biochemistry 23*, 1555–1563.
Stein, L. A., Greene, L. E., Chock, P. B., & Eisenberg, E. (1985) *Biochemistry 24*, 1357–1363.
Stein, L. A., Evans, J. A., & Eisenberg, E. (1989) *Biochemistry* (following paper in this issue).
Swanson, J. R., & Yount, R. G. (1966) *Biochem. Z. 345*, 395–409.
von der Saal, W., Crysler, C. S., & Villafranca, J. J. (1985) *Biochemistry 24*, 5343–5350.
White, D. C. S., Ricigliano, J. W., & Webb, M. R. (1987) *J. Muscle Res. Cell Motil. 8*, 537–540.
Yount, R. G., Babcock, D., Ballantyne, Wm., & Ojala, D. (1971) *Biochemistry, 10*, 2484–2489.

Oxygen Exchange Kinetics of Porcine Cardiac Acto–Subfragment 1†

Leonard A. Stein, John A. Evans, and Evan Eisenberg*
Laboratory of Molecular Cardiology, Department of Medicine, SUNY at Stony Brook, Stony Brook, New York 11794, and Laboratory of Cell Biology, National Heart, Lung, and Blood Institute, National Institutes of Health, Bethesda, Maryland 20892

Received December 19, 1988; Revised Manuscript Received May 30, 1989

ABSTRACT: Recent studies have shown that the K_{ATPase} of porcine cardiac S-1 is severalfold stronger than $K_{binding}$. As with skeletal S-1, the four-state model can only explain this observation with the assumption that the release of the products of hydrolysis is rapid and not rate limiting. However, if the release of products is fast, the four-state model predicts that the extent of oxygen exchange with porcine cardiac S-1 should fall toward zero at high actin concentrations, as previously observed with skeletal acto–S-1. In the current work, we show that, in fact, the extent of oxygen exchange for porcine cardiac S-1 remains significant even at infinite actin concentration (i.e., with cross-linked actin–S-1) and that, therefore, the four-state model cannot adequately account for the oxygen exchange data and the ratio of $K_{binding}$ to K_{ATPase} simultaneously. As in the skeletal case, in order for the six-state model to account for these data, it is necessary to assume that P_i rotation in the acto–S-1·ADP·P_i state is rate limiting for oxygen exchange.

During the last 2 decades, there has been a great deal of interest in the biochemical kinetics of the skeletal myosin subfragment 1 (S-1)[1] ATPase activity (Taylor, 1979; Eisenberg & Greene, 1980; Sleep & Smith, 1981; Webb & Trentham, 1983). This work has led to the development of two possible models for the actin activation of the S-1 ATPase activity, a four-state model and a six-state model (Figure 1) (Stein et al., 1981). While there is a general consensus that a four-state model is the minimal kinetic model which can explain the actomyosin ATPase activity, there is still controversy over whether this model can actually account for all of the available steady-state and pre-steady-state data (Stein, 1988).

Data that are central to the argument against a four-state model are the difference observed between K_{ATPase}, the actin concentration where half-maximal acto–S-1 ATPase activity occurs, and $K_{binding}$, the actin concentration where half-maximal binding of the S-1–ATP complex to actin occurs. Stein et al. (1981) had noted a 4–8-fold difference between these constants for the skeletal myosin isoenzyme (A-1)S-1, and when the four-state and six-state models are required to account for this difference, they predict very different magnitudes of the phosphate burst at infinite actin concentration (Stein et al., 1984). The four-state model predicts that the magnitude of the P_i burst will fall toward zero as the actin concentration is increased, while the six-state model predicts that there will be a significant burst magnitude even at saturating actin concentration. Unfortunately, measurement of the magnitude of the phosphate burst at high actin concentrations is very difficult, and, therefore, there is still controversy over whether this magnitude is consistent with the four-state or the six-state model (Stein, 1988).

The reason that the four-state model predicts a very low value for the magnitude of the P_i burst at high actin concentrations is that this model can only account for the large difference between K_{ATPase} and $K_{binding}$ if the ATP hydrolysis step with actin bound is rate limiting and the P_i release step is very rapid. The four-state model therefore predicts that, during steady-state hydrolysis of ATP, state A·M·ADP·P_i will decompose much more rapidly than it is formed and will not be occupied to a significant extent. If state A·M·ADP·P_i is not occupied to a significant degree, the four-state model also leads to the prediction that almost no ^{18}O exchange should occur at high actin concentration. ^{18}O exchange requires that many reversals occur between state A·M·ADP·P_i and A·M·ATP before P_i is released into the solution. If the P_i release step is very rapid compared to the reverse rate of the ATP hydrolysis step, P_i release will occur before any reversals of the ATP hydrolysis step can take place, and, therefore, no ^{18}O

†This work was supported by National Institutes of Health Grant RO1-HL32962 as well as by a Suffolk Heart Association grant, both awarded to L.A.S. L.A.S. is also the recipient of a Research Career Development award from the NIH.

[1] Abbreviations: S-1, myosin subfragment 1; A, actin; V_{max}, maximal ATPase rate per myosin residue; K_{ATPase}, actin concentration where half the maximal ATPase rate (V_{max}) is achieved; $K_{binding}$, actin concentration necessary to achieve half S-1 bound, during steady-state hydrolysis of ATP; M, myosin subfragment 1; P_i, inorganic phosphate; ATP, adenosine 5′-triphosphate.

0006-2960/89/0428-7747$01.50/0

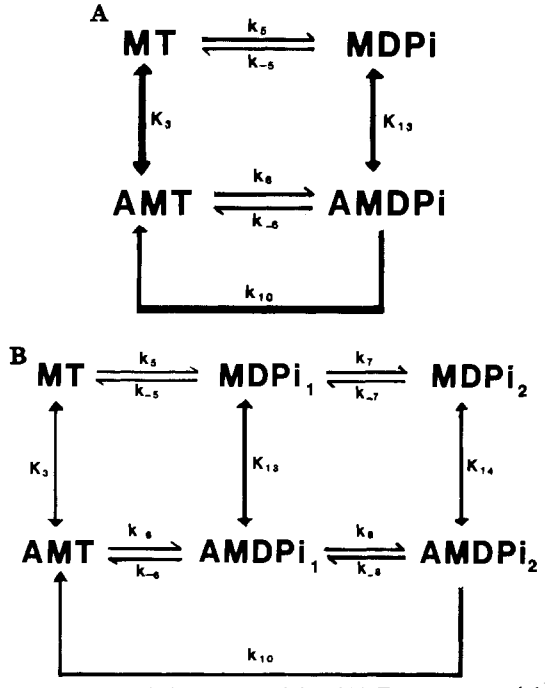

FIGURE 1: Four- and six-state models. (A) Four-state model; (B) six-state model. In these models, A = actin, M = S-1, T = ATP, D = ADP, and P_i = inorganic phosphate. In both models, the dissociation constants K_3, K_{13}, and K_{14} are assumed to represent rapid equilibria.

exchange will take place at high actin concentration.

In the present study, using porcine cardiac myosin, we tested whether there is a correlation between a large difference between K_{ATPase} and $K_{binding}$ and a low level of ^{18}O exchange at high actin concentration as predicted by the four-state kinetic model. A recent comparative study of porcine cardiac and rabbit skeletal S-1 (Stein & White, 1987) revealed that these two proteins are kinetically very similar except that the porcine cardiac S-1 has a lower maximal actin-activated ATPase activity. In particular, at low ionic strength, porcine cardiac S-1 showed a 4–6-fold difference between K_{ATPase} and $K_{binding}$, which predicts, if the four-state model is valid, that the level of ^{18}O exchange should approach zero at high actin concentrations. In fact, in contrast to the situation with skeletal muscle S-1, we find that the level of ^{18}O exchange with cardiac S-1 remains high at high actin concentrations. These data suggest that the four-state kinetic model is not adequate to explain the kinetic behavior of porcine cardiac acto–S-1. The six-state kinetic model can explain these data but only if it is assumed that slow P_i rotation limits the amount of ^{18}O exchange which occurs at high actin concentrations.

Materials and Methods

Proteins. Porcine cardiac subfragment 1 was prepared from adult pigs as described previously (Stein & White, 1987). Rabbit skeletal actin was prepared as described previously (Eisenberg & Keilley, 1974). Cross-linked actin–S-1 was prepared by the method of Mornet et al. (1981) as described previously (Stein & White, 1987). ^{18}O analysis was carried out as described previously (Evans & Eisenberg, 1989). Steady-state ATPase activities were measured by mixing actin, S-1, ATP, etc. in a 5-mL thermostated beaker and following the hydrolysis of ATP either by using pH-stat techniques (Stein et al., 1979) with a radiometer titration system or by using [γ-^{32}P]ATP and assaying for hydrolyzed P_i as described previously (Stein & White, 1987). Quench-flow and stopped-flow studies were carried out as described previously (Stein et al., 1979) except that machines designed by Dr. Ken Johnson at Penn State University were employed. Binding experiments were carried out using "airfuge" techniques essentially as described previously (Chalovich et al., 1984), in which actin, S-1, and ATP are mixed under temperature-controlled conditions and then during the steady-state hydrolysis of ATP the mixture is rapidly spun in a Beckman ultracentrifuge at approximately 100000g to pellet the acto–S-1 complexes.

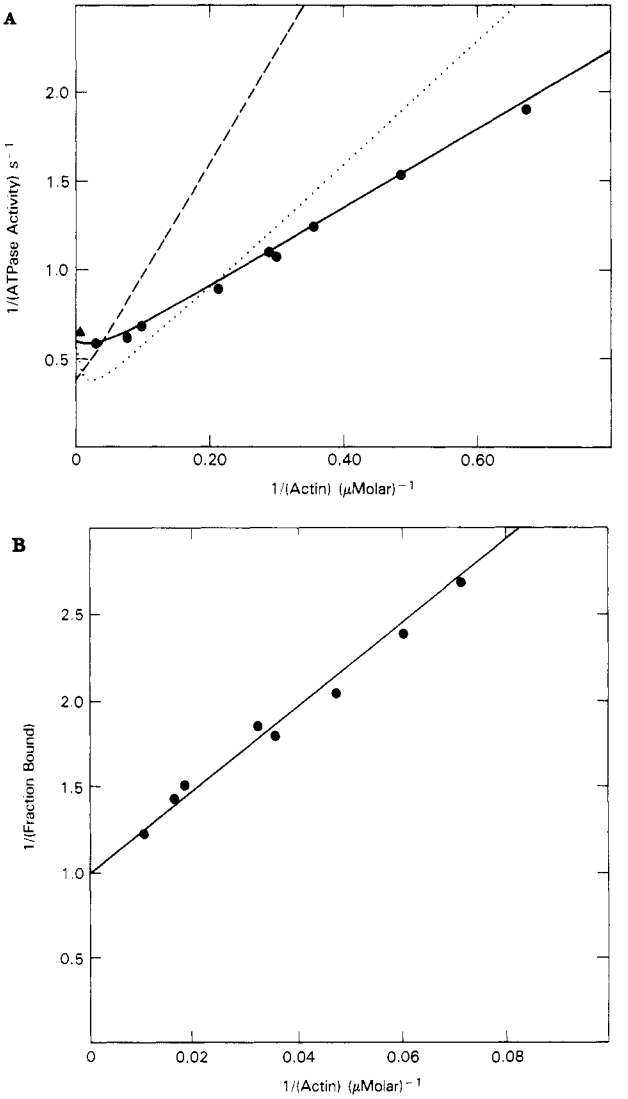

FIGURE 2: Determination of K_{ATPase} and $K_{binding}$. (A) Determination of V_{max} and K_{ATPase}: (●) data with acto-S-1; (▲) data with cross-linked actin–S-1. Conditions: 10 mM imidazole, 1 mM MgATP, and 1 mM $MgCl_2$, pH 7, 15 °C. The line drawn through the data is the prediction of the six-state model with $k_5 = 16\ s^{-1}$, $k_{-5} = 8\ s^{-1}$, $k_6 = 26\ s^{-1}$, $k_{-6} = 39\ s^{-1}$, $k_7 = 5\ s^{-1}$, $k_{-7} = 50\ s^{-1}$, $k_8 = 5\ s^{-1}$, $k_{-8} = 50\ s^{-1}$, $k_{10} = 300\ s^{-1}$, $K_3 = 14\ \mu M$, and $K_{13} = K_{14} = 42\ \mu M$. Theoretical plots for the four-state model: (dashed plot) $k_5 = 16\ s^{-1}$, $k_{-5} = 8\ s^{-1}$, $k_6 = 5.5\ s^{-1}$, $k_{-6} = 22\ s^{-1}$, $k_{10} = 22\ s^{-1}$, $K_3 = 12\ \mu M$, and $K_{13} = 96\ \mu M$; (dotted plot) $k_5 = 16\ s^{-1}$, $k_{-5} = 8\ s^{-1}$, $k_6 = 2\ s^{-1}$, $k_{-6} = 3\ s^{-1}$, $k_{10} = 20.5\ s^{-1}$, $K_3 = 16\ \mu M$, and $K_{13} = 48\ \mu M$. (B) Binding of actin to S-1 during steady-state hydrolysis of ATP. Conditions as in (a). The line drawn through the data is the best fit with the requirement that the fraction bound is 1.0 at infinite actin concentration.

Results

Figure 2A shows a double-reciprocal plot of cardiac S-1 ATPase activity vs actin concentration. Extrapolation of the plot to infinite actin concentration gives a V_{max} value of 2 s^{-1}, which is about half the value of V_{max} observed for skeletal S-1 under the same condition. The solid triangle on the ordinate

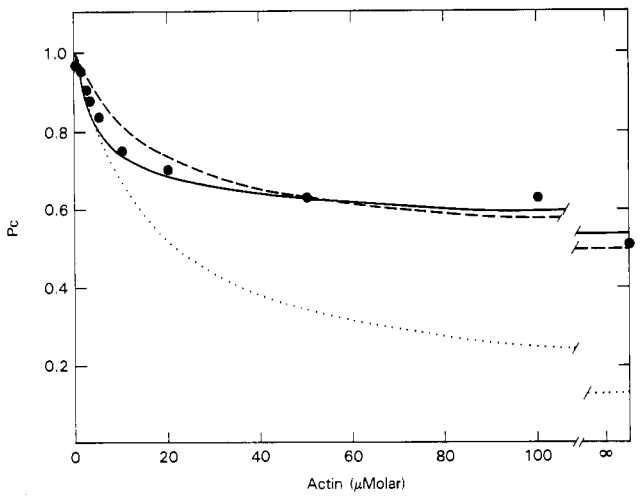

FIGURE 3: ^{18}O exchange kinetics: P_c as a function of the actin concentration. The point at infinite actin concentration was determined with cross-linked actin–S-1. Conditions as in Figure 2. The solid line drawn through the data is the prediction of the six-state model with rate constants as in Figure 2. The dashed and dotted lines are predictions of the four-state model; rate constants as given in Figure 2.

shows the ATPase activity with cross-linked S-1; as has been noted previously, this rate is less than the extrapolated V_{max}, possibly because of partial denaturation of the cross-linked S-1 or possibly because of inhibition of the ATPase activity at saturating actin concentrations as has been observed in the past (Stein et al., 1985; Stein, 1988). The abscissa intercept gives a value for K_{ATPase} of 4.5 μM, similar to the value of K_{ATPase} observed with skeletal acto–S-1 under this condition.

Figure 2B shows a double-reciprocal plot of the fraction of S-1 bound to actin vs the actin concentration. The abscissa intercept gives a value for $K_{binding}$ of 24 μM. These data confirm the previous result from this laboratory showing about a 5-fold difference between K_{ATPase} and $K_{binding}$ for porcine cardiac acto–S-1. However, this may not be the case for all cardiac myosins, since K_{ATPase} and $K_{binding}$ have been reported to be only about 2-fold different with bovine cardiac S-1 (White & Hackney, 1987).

As we discussed previously, the four-state kinetic model can only explain a 5-fold difference in K_{ATPase} and $K_{binding}$ if P_i release is assumed to be fast and the ATP hydrolysis step, itself, is rate limiting. This in turn predicts, as in the case of skeletal S-1, that very little ^{18}O exchange should occur with cardiac S-1 at high actin concentration. Figure 3 shows a plot of the measured P_c (see Appendix) for cardiac acto–S-1 plotted as a function of the actin concentration. The point at infinite actin concentration was performed with EDC-cross-linked acto–S-1. At zero actin, P_c equals 0.97, and P_c then falls rapidly to reach a value of approximately 0.5 at infinite actin concentration, a considerably higher value than occurs with skeletal S-1. Therefore, as has been reported for bovine cardiac S-1 (White & Hackney, 1987), at high actin concentration considerably more ^{18}O exchange appears to occur with cardiac S-1 than with skeletal S-1. To be certain that the ^{18}O exchange experiments could be validly compared to similar experiments with skeletal S-1, we checked that, at all of the actin concentrations studied, the cardiac S-1 showed a single pathway of ^{18}O exchange. Figure 4 shows that a single pathway of ^{18}O exchange adequately accounts for the data observed under all conditions studied.

Before determining whether the four-state model could fit both our ^{18}O exchange data and ATPase data, we also measured the tryptophan fluorescence enhancement rate as a

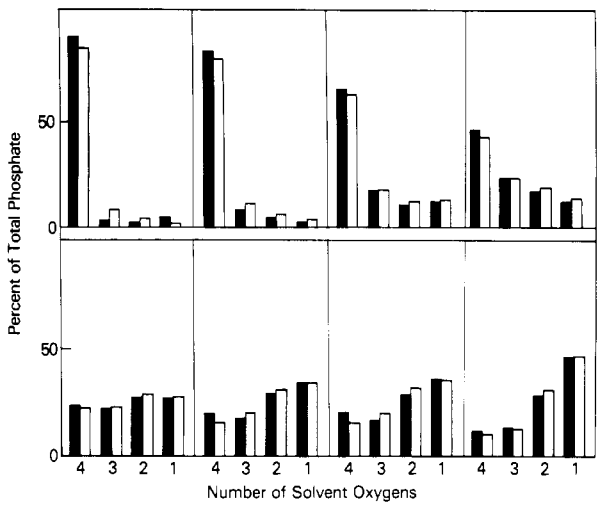

FIGURE 4: Distribution of phosphate species: actin concentration dependence. S-1 (0.1–0.4 μM) was incubated in a 13 mM ionic strength buffer containing (in mM) 2 imidazole, 1 [^{18}O]ATP, 1 DTT, 4.5 KCl, and the indicated concentration of actin in a beaker thermostated to 15 °C. The ATPase rate was determined by pH-stat titration at pH 7.0. Upon completion of the reaction, the P_i was isolated, and the distribution of oxygen isotopes was determined as performed previously (see Materials and Methods). The solid bars represent the observed percentage of phosphate molecules containing from four to one atom of oxygen from the medium water. These percentages were summed to yield an average number of water oxygens per phosphate which is related to P_c (see Materials and Methods). The open bars are the theoretical distributions assuming a single path of hydrolysis. Actin concentrations (in μM): (top) 0.0, 1.0, 2.5, and 5.0; (bottom) 20, 50, 100, and cross-linked.

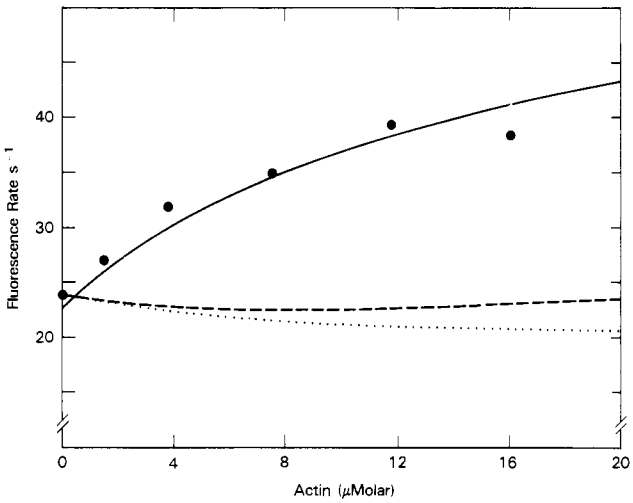

FIGURE 5: Tryptophan fluorescence rate. Conditions as in Figure 2. The solid line is the prediction of the six-state model with rate and binding constants as given in Figure 2. Both the dashed and dotted lines are the predictions of the four-state model with constants as given in Figure 2.

function of the actin concentration (Figure 5). Referring to the Appendix and Figure 1A, the fluorescence rate in the absence of actin is given by $k_5 + k_{-5}$, and in the presence of actin, the fluorescence rate is the rate constant for the approach of the system to the steady state, and its analytical form is model dependent. However, any model being considered for the actin-activated myosin ATPase activity should be able to account for the fluorescence enhancement data. The results show that, as with skeletal S-1, the fluorescence enhancement rate of porcine cardiac S-1 increases as the actin concentration is increased and at high actin concentrations the fluorescence rate appears to be extrapolating to a maximum of about 40–50 s^{-1}. In fitting our data to the four-state model, we first at-

tempted to fit the ATPase data. The rate constants k_5 and k_{-5} are generally determined from the fluorescence enhancement rate in the absence of actin (i.e., $k_5 + k_{-5} = 24\ s^{-1}$) and the fact that the equilibrium constant K_5 (k_5/k_{-5}) is generally found to be in the range of 2–3 using quench-flow techniques, and has been assumed to be 2 in the present case (Stein & White, 1987; Stein et al., 1989). As we discussed in an earlier paper, the difference noted between K_{ATPase} and $K_{binding}$ can only be explained by the four-state model if k_6 is rate limiting and k_{10} is relatively fast (Stein et al., 1981). The dotted line in Figure 2 shows the closest we could come to fitting the ATPase data. In this fit, we set the rate of the hydrolysis step, k_6, equal to 2 s^{-1} (which is required to limit the ATPase rate at infinite actin), and we set the rate of the P_i release step, k_{10}, equal to 20.5 s^{-1} (which gave the best fit to the data). The resulting fit to the ATPase data was reasonable but not perfect because it predicted a higher ATPase rate at high actin concentration than was obtained experimentally. A similar reasonable but imperfect fit was obtained when the skeletal S-1 ATPase data were fit to the four-state model (Stein et al., 1981). The dotted line in Figure 3 shows how this set of rate constants fits the ^{18}O exchange data. As can be seen, this model fits the ^{18}O exchange data very poorly, predicting that the amount of ^{18}O exchange should drop to a very low level at infinite actin concentration.

It is not surprising that the dotted line in Figure 3 did not fit the ^{18}O exchange data. To explain the P_c value of 0.5 at saturating actin concentration, k_{-6} must be set equal to k_{10} (see Figure 1A), and in the dashed plot, k_{10}/k_{-6} is approximately 7. Therefore, we next attempted to fit the ^{18}O exchange data by setting k_{-6} equal to k_{10}, at the same time keeping k_{10} as large as possible compared to k_6 to explain the difference between K_{ATPase} and $K_{binding}$. The dashed lines in Figures 2 and 3 show the results of this fit. Since we set k_{-6} equal to k_{10}, we were able to account for the ^{18}O exchange data. However, we could not fit the 5-fold difference between K_{ATPase} and $K_{binding}$ even though k_{10} was 4-fold larger than k_6. The dashed line in Figure 2 has a K_{ATPase} value less than 2-fold stronger than $K_{binding}$. The difficulty encountered is that increasing the value of both k_{-6} and k_{10} increases the difference between k_6 and k_{10} but does not strengthen K_{ATPase}. The reason for this is that the ratio of k_6 to k_{-6} falls as k_{-6} and k_{10} are increased, and by detailed balance, the dissociation constant K_{13} must be made weaker, negating the effect of a faster k_{10}. Note that even the relatively poor fit which we obtained still requires K_{13} to be 8-fold weaker than K_3, considerably larger than the 3-fold difference generally assumed for the difference in the binding of M·ATP and M·ADP·P_i to actin.

Not only is the four-state model unable to simultaneously fit both the ATPase data and the ^{18}O exchange data, in addition it is unable to fit the fluorescence enhancement data. The dotted and dashed lines in Figure 5 show that whether we used the set of rate constants that fit the ATPase data (dotted line) or the set of constants that fit the ^{18}O exchange data (dashed line), the results were essentially the same. In both cases, we were unable to fit the increase in the fluorescence rate that occurs at low actin concentration. The problem is that the value of k_{10} is too low to make the rate of fluorescence enhancement increase at low actin concentration. Furthermore, it is not possible to increase the value of k_{10} because with the set of rate constants that fit the ATPase activity, the ATPase activity would become too high at low actin concentrations, while with the set of rate constants that fit the oxygen exchange data, as noted above, the accompanying increase in k_{-6} and the weakening of K_{13} will negate the effect of increasing k_{10}. Therefore, the four-state model does not seem to be able to account for the increase in the fluorescence enhancement rate which occurs at low actin concentration.

We next attempted to fit the data in Figures 2, 3, and 5 to the six-state model. As can be seen (solid lines in Figures 2, 3, and 5), the fit is generally quite good. However, as with skeletal muscle S-1, to fit the oxygen exchange data we found it necessary to assume that rotation of P_i in the state A·M·ADP·P_i is rate limiting for exchange (Bagshaw & Trentham, 1975). In other words, the reverse transition A·M·ADP·$P_i \rightarrow$ A·M·ATP is fast in comparison to the rate of rotation of the terminal phosphate, and, therefore, the reverse rate constant for exchange is only a fraction of the actual reverse rate. To fit the ^{18}O exchange data in Figure 3, we assumed that the overall rate of exchange was 5 s^{-1}, meaning that the rate of rotation of the P_i was about 6 s^{-1} while the rate of the transition from A·M·ADP·P_i to A·M·ATP was about 39 s^{-1}.

Discussion

In the present paper, we tested whether the four-state kinetic model can account for the kinetic properties of the porcine cardiac actomyosin ATPase activity or whether a six-state model is necessary. The major difference between the four-state and six-state models is the nature of the rate-limiting step in the ATPase cycle. Since the rate-limiting step controls the velocity of muscle contraction, it is important to know whether the rate-limiting step is the ATP hydrolysis step (4-state model) or a separate rate-limiting step which follows the ATP hydrolysis step and has the same rate whether or not S-1 is bound to actin (six-state model).

There is general agreement that, in order for the four-state model to account for the difference between K_{ATPase} and $K_{binding}$ which occurs with skeletal muscle S-1, the rate of the P_i release step must be rapid compared to the rate of the ATP hydrolysis step. Therefore, the four-state model predicts that state A·M·ADP·P_i should exist in low concentration compared to state A·M·ATP. This, in turn, leads to the prediction that, at saturating actin concentration, both the initial P_i burst and the steady-state ^{18}O exchange will be very low.

Both of these predictions of the four-state kinetic model have been tested with skeletal muscle S-1. Unfortunately, there is disagreement about the magnitude of the P_i burst with skeletal muscle acto–S-1, and this is at least partially due to the difficulty associated with the burst measurement at high actin concentrations (Stein et al., 1985; Rosenfeld & Taylor, 1984). However, it is clear that, at saturating actin concentration, the level of ^{18}O exchange is very low with skeletal muscle S-1, just as is predicted by the four-state model (Webb & Trentham, 1982).

In the present paper, we studied the amount of ^{18}O exchange which occurs with porcine cardiac S-1. We used porcine cardiac S-1 because it shows the same difference between K_{ATPase} and $K_{binding}$ that is shown by skeletal muscle S-1. Of course, some variability does exist in various preparations of cardiac S-1. At 15 °C and low ionic strength, the V_{max} for cardiac S-1 has been consistently in the range of 1.7–2.2 s^{-1} with about 20 different protein preparations. K_{ATPase} has also been found to be consistently in the range of 3–6 μM while different preparations gave values for $K_{binding}$ in the range of 20–25 μM using airfuge techniques and 30–40 μM with light-scattering methods (Stein & White, 1987; Stein et al., 1989). When determined on the same protein preparation, the ratio of $K_{binding}$ to K_{ATPase} has always been at least 4. Therefore, we are certain that with porcine cardiac S-1, the difference between K_{ATPase} and $K_{binding}$ is similar to what is

observed with skeletal muscle S-1. However, this may not be the case for all cardiac myosins since bovine cardiac S-1 has been reported to show only about a 2-fold difference between K_{ATPase} and $K_{binding}$ (White & Hackney, 1987).

Given our observation that the difference between K_{ATPase} and $K_{binding}$ is nearly the same for porcine cardiac S-1 and for skeletal muscle S-1, the four-state kinetic model predicts that porcine cardiac S-1 should show the same low ^{18}O exchange at high actin concentration as skeletal S-1. In fact, our data clearly show that much more ^{18}O exchange occurs with cardiac S-1 at high actin concentration than occurs with skeletal S-1. Likewise, cardiac S-1 cross-linked to actin shows much more ^{18}O exchange than cross-linked skeletal acto–S-1. Bovine cardiac S-1 has also been reported to show considerably more ^{18}O exchange at high actin concentration than does skeletal S-1 (White & Hackney, 1987).

Attempts to simultaneously fit both the observed difference between K_{ATPase} and $K_{binding}$ and the ^{18}O exchange data to the four-state model were not successful. In addition, we were unable to fit the fluorescence data to the four-state model. As with skeletal S-1, experimentally the rate of the fluorescence enhancement increases with increasing actin concentration at low actin concentrations, but the four-state kinetic model actually predicts that the rate of the fluorescence enhancement is biphasic as a function of actin concentration, decreasing at low actin concentrations and then increasing at much higher actin concentrations. This behavior is caused by the relatively low value of k_{10} required in the four-state model to fit the value of V_{max} consistently observed with cardiac S-1. Only if V_{max} were as high as it is with skeletal muscle S-1 could the fluorescence data be fit more satisfactorily by the four-state kinetic model. This can also be seen more mathematically as follows: According to the four-state model, the fluorescence enhancement rate is given by $k_5' + k_{-5}' + k_6' + k_{-6}' + k_{10}'$, where the primed rate constants are defined in the Appendix. Here it can be seen that $k_5' + k_{-5}' = k_5K_3/(K_3 + [A]) + k_{-5}K_{13}/(K_{13} + [A])$ which is equal to $k_5 + k_{-5}$ at zero actin, but decreases as a function of the actin concentration. It can also be appreciated that $k_6' + k_{-6}' + k_{10}' = k_6[A]/(K_3 + [A]) + (k_{-6} + k_{10})[A]/(K_{13} + [A])$ and that this sum is zero at zero actin and increases as a function of the actin concentration. Clearly then, the sum of such terms will in general give a biphasic plot unless the rise of the second term is greater than the fall of the first as a function of actin concentration, which is not the case here.

The poor fit to our data which we obtained with the four-state kinetic model shows that this minimal model, which just managed to fit the skeletal muscle S-1 data, is unable to fit the porcine cardiac S-1 data. On the other hand, the six-state kinetic model is able to adequately fit these data. This is not surprising since the six-state model has more degrees of freedom than the four-state model. However, in order to fit the ^{18}O exchange data to the six-state model, it is necessary to assume that there is restriction to rotation of P_i at the active site. Otherwise, as in the skeletal system, the six-state model predicts that too much ^{18}O exchange will occur at high actin concentrations.

In conclusion, the four-state model can account for the ATPase activity of cardiac S-1 including the rate of the cross-linked actin–S-1 and the ^{18}O exchange data individually, but not simultaneously. In addition, the four-state model does not appear to be able to account for the fluorescence rate data unless the value of V_{max} is as high with cardiac myosin as with skeletal myosin. In contrast to the four-state model, the six-state model can account for the data, but to account for the oxygen exchange data, it is necessary to assume that the effective reverse rate for oxygen exchange is considerably less than the kinetic reverse rate due to rate limitation in the rotation of the terminal P_i in state A·M·ADP·P_i.

Scheme I

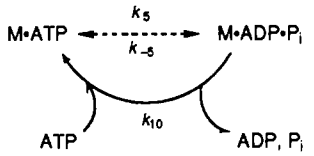

Appendix

In this section, the theoretical equations that were used to analyze the data will be presented and discussed.

Four-State Model

^{18}O Exchange. Consider Scheme I for the hydrolysis of ATP by myosin in the absence of actin where P_i = inorganic phosphate. It has been assumed here that the ATP is at saturating concentrations (>0.5 mM). In order to relate the rate constants to the predicted ^{18}O exchange, it is necessary to make two assumptions. First, it is necessary to assume that the terminal P_i of the ATP molecule in the state M·ADP·P_i is free to rotate. Second, it is necessary to assume that the rotation rate of the P_i moiety in the state M·ADP·P_i is much faster than the back-rate k_{-5}. If these conditions are satisfied, then a study of the ^{18}O exchange during steady-state hydrolysis of ATP will lead to an O/P ratio given by (Sleep et al., 1978; Hackney, 1980):

$$O/P = 4/\{1 + 3[k_+/(k_+ + k_-)]\}$$

where in this case $k_- = k_{-5}$ and $k_+ = k_{10}$.

In the presence of actin, the system becomes somewhat more complex, although obvious similarities exist. Consider the four-state model (Figure 1). In order to use the equation above for the O/P ratio, we must assign values for the forward rate, k_+, and for the backward rate, k_-. In the equation above, k_+ is the net forward rate, and k_- is the rate constant for return from the states A·M·ADP·P_i + M·ADP·P_i to A·M·ATP + M·ATP. Assuming that K_{13} represents a rapid equilibrium and that therefore the states A·M·ADP·P_i + M·ADP·P_i can be treated as a single state, the net outward rate constant predicted by the four-state model is given by

$$k_+ = k_{10}[\text{actin}]/(K_{13} + [\text{actin}])$$

and the reverse rate constant can be written as

$$k_- = (k_{-5}K_{13} + k_{-6}[\text{actin}])/(K_{13} + [\text{actin}])$$

While these are correct expressions for the forward and reverse rate constants according to the four-state model, they cannot be used in the above expression for the O/P ratio unless it is assumed that P_i rotation in the reverse transition is both free and not rate limiting. At saturating actin, $k_+ = k_{10}$, and $k_- = k_{-6}$, and the O/P ratio under these conditions is given by $4/\{1 + 3[k_{10}/(k_{10} + k_{-6})]\}$. The degree of exchange is often described by the ratio $k_-/(k_- + k_+)$, which is called P_c, instead of the actual O/P ratio. The two expressions are related by $O/P = 4/[1 + 3(1 - P_c)]$.

ATPase Activity. Assuming that K_3 and K_{13} represent rapid equilibria, the steady-state ATPase activity predicted by the four-state model can be written as (Stein et al., 1979)

$$V_{ss} = (k_5' + k_6')k_{10}'/(k_5' + k_6' + k_{-5}' + k_{-6}' + k_{10}')$$

where $k_5' = k_5K_3/(K_3 + [\text{actin}])$, $k_6' = k_6[\text{actin}]/(K_3 + [\text{actin}])$, $k_{-5}' = k_{-5}K_{13}/[K_{13}/(K_{13} + [\text{actin}])]$, $k_{-6}' = k_{-6}[\text{actin}]/(K_{13} + [\text{actin}])$, and $k_{10}' = k_{10}[\text{actin}]/(K_{13} + [\text{actin}])$.

At saturating actin, the ATPase activity is given by

$$V_{ss}([\text{actin}]\rightarrow\text{infinity}) = k_6k_{10}/(k_6 + k_{-6} + k_{10})$$

Tryptophan Fluorescence Rate. Referring to the model for the ATPase activity of S-1 in the absence of actin given in Scheme I, when ATP is added to myosin an enhancement of the intrinsic tryptophan fluorescence occurs in the transition from M·ATP to M·ADP·P_i. This transition occurs with a rate constant given by $k_5 + k_{-5}$. Assuming the four-state model, in the presence of actin, the rate of the tryptophan fluorescence is given by (Stein et al., 1981)

$$\text{rate} = k_5' + k_6' + k_{-5}' + k_{-6}' + k_{10}'$$

Six-State Model

Referring to Figure 1, and with the additional definitions $k_7' = k_7K_{13}/(K_{13} + [\text{actin}])$, $k_{-7}' = k_{-7}K_{14}/(K_{14} + [\text{actin}])$, $k_8' = k_8[\text{actin}]/K_{13} + [\text{actin}])$, and $k_{-8}' = k_{-8}[\text{actin}]/(K_{14} + [\text{actin}])$ plus the fact that the six-state model k_{10}' is redefined as

$$k_{10}' = k_{10}[\text{actin}]/(K_{14} + [\text{actin}])$$

the analytical expressions predicted by the six-state model are as follows.

Oxygen Exchange. Let

$$k_- = f_1k_{-5}' + f_2k_{-6}'$$

$$k_+ = (k_7' + k_8')k_{10}'/(k_{-7}' + k_{-8}' + k_{10}')$$

In the expression for k_-, two multiplicative factors (f_1 and f_2) have been introduced to allow for the possibility that rotation of the terminal phosphate in the states M·ADP·P_i and A·M·ADP·P_i is inhibited, and therefore the back-rate for exchange must be reduced.

ATPase Activity. Let

$$A = k_{10}'(k_5' + k_6')(k_7' + k_8')$$

and

$$B = (k_{10}' + k_5' + k_6')(k_7' + k_8') + (k_{10}' + k_{-7}' + k_{-8}')(k_5' + k_6' + k_{-5}' + k_{-6}')$$

then $1/V_{ss} = A/B$.

Fluorescence Rate. The six-state model has two relaxation rates associated with it. In general, the conditions are chosen so that one of the rates is very rapid, and, therefore, this portion of the transient is over within the dead time of the apparatus. Let $A_1 = k_{-7}' + k_{-8}' - k_5' - k_6'$, $A_2 = k_{-7}' + k_{-8}' + k_{10}'$, $B_1 = k_{-5}' + k_{-6}' + k_5' + k_6' + k_7' + k_8'$, and $B_2 = k_7' + k_8'$, then the rate constants are given by

$$(B_1 + A_2)/2 + \{[(B_1 + A_2)^2 + 4(A_1B_2 - A_2B_1)]^{1/2}\}/2$$

References

Bagshaw, C., & Trentham, D. R. (1975) *J. Supramol. Struct. 3*, 315–322.

Chalovich, J. M., Stein, L. A., Greene, L. E., & Eisenberg, E. (1984) *Biochemistry 23*, 4885–4890.

Eisenberg, E., & Keilley, W. W. (1974) *J. Biol. Chem., 249*, 4742–4750.

Eisenberg, E., & Greene, L. E. (1980) *Annu. Rev. Physiol. 42*, 921–956.

Evans, J. A., & Eisenberg, E. (1989) *Biochemistry* (preceding paper in this issue).

Hackney, D. D. (1980) *J. Biol. Chem. 255*, 5320–5328.

Marston, S. B., & Taylor, E. W. (1980) *J. Mol. Biol. 139*, 573–600.

Mornet, D., Bertrand, R., Pantel, P., Audemard, E., & Kassab, R. (1981) *Nature 292*, 301–306.

Rosenfeld, S. S., & Taylor, E. W. (1984) *J. Biol. Chem. 259*, 11908–11919.

Sleep, J. A., & Smith, S. J. (1981) *Curr. Top. Bioenerg. 2*, 121.

Sleep, J. A., Hackney, D. D., & Boyer, P. D. (1978) *J. Biol. Chem. 253*, 5235.

Stein, L. A. (1988) *Cell Biophys. 12*, 29–58.

Stein, L. A., & White, M. P. (1987) *Circ. Res. 60*, 39–49.

Stein, L. A., Schwartz, R., Chock, P. B., & Eisenberg, E. (1979) *Biochemistry 18*, 3895–3909.

Stein, L. A., Chock, P. B., & Eisenberg, E. (1981) *Proc. Natl. Acad. Sci. U.S.A. 78*, 1346–1350.

Stein, L. A., Chock, P. B., & Eisenberg, E. (1984) *Biochemistry 23*, 1555–1563.

Stein, L. A., Greene, L. E., Chock, P. B., & Eisenberg, E. (1985) *Biochemistry 24*, 1357–1363.

Stein, L. A., White, M. P., & Annis, D. T. (1989) *Circ. Res.* (in press).

Taylor, E. W. (1979) *CRC Crit. Rev. Biochem. 4*, 103–164.

Webb, M. R., & Trentham, D. R. (1982) *Fed. Proc., Fed. Am. Soc. Exp. Biol. 41*, 1417.

Webb, M. R., & Trentham, D. R. (1983) *Handb. Physiol. 10*, 237–255.

White, H., & Hackney, D. D. (1987) *Biophys. J. 51*, p28a.